Songklanakarin J. Sci. Technol.
34 (4), 415-421, Jul. - Aug. 2012

SONGKLANAKARIN JOURNAL OF SCIENCE AND TECHNOLOGY
http://www.sjst.psu.ac.th

Original Article

Influence of friction stir welding parameters on metallurgical and mechanical properties of dissimilar joint between semi-solid metal 356-T6 and aluminum alloys 6061-T651

Muhamad Tehyo[1]*, Prapas Muangjunburee[2], Abdul Binraheem[1], Somchai Chuchom[3] and Nisida Utamarat[1]

[1] *Department of Industrial Engineering, Faculty of Engineering, Princess of Naradhiwas University, Mueang, Narathiwat, 96000 Thailand.*

[2] *Department of Mining and Materials Engineering,*

[3] *Department of Industrial Engineering, Faculty of Engineering, Prince of Songkla University, Hat Yai, Songkhla, 90112 Thailand.*

Received 3 November 2011; Accepted 4 June 2012

Abstract

The objective of this research is to investigate the effect of welding parameters on the microstructure and mechanical properties of friction stir (FS) welded butt joints of dissimilar aluminum alloy sheets between Semi-Solid Metal (SSM) 356-T6 and AA6061-T651 by a computerized numerical control (CNC) machine. The base materials of SSM356-T6 and AA6061-T651 were located on the advancing side (AS) and on the retreating side (RS), respectively. For this experiment, the FS welded materials were joined under two different tool rotation speeds (1,750 and 2,000 rpm) and six welding speeds (20, 50, 80, 120, 160, and 200 mm/min), which are the two prime joining parameters in FSW. From the investigation, the higher tool rotation speed affected the weaker material's (SSM) maximum tensile strength less than that under the lower rotation speed. As for welding speed associated with various tool rotation speeds, an increase in the welding speed affected lesser the base material's tensile strength up to an optimum value; after which its effect increased. Tensile elongation was generally greater at greater tool rotation speed. An averaged maximum tensile strength of 206.3 MPa was derived from a welded specimen produced at the tool rotation speed of 2,000 rpm associated with the welding speed of 80 mm/min. In the weld nugget, higher hardness was observed in the stir zone than that in the thermo-mechanically affected zone. Away from the weld nugget, hardness levels increased back to the levels of the base materials. The microstructures of the welding zone in the FS welded dissimilar joint can be characterized both by the recrystallization of SSM356-T6 grains and AA6061-T651 grain layers.

Keywords: SSM356-T6, AA6061-T651, friction stir welding (FSW), dissimilar joint

1. Introduction

In recent years, demands for light-weight and/or high-strength sheet metals such as aluminum alloys have steadily increased in aerospace, aircraft, and automotive applications because of their excellent strength to weight ratio, good ductility, corrosion resistance and cracking resistance in adverse environments. Semi-solid metals (SSM), mostly aluminum alloys, have emerged in the usage of casting components in various applications. Joining between SSM356-T6 casting aluminum alloy and AA6061-T651 is a common combination that requires good strength joints and an easy process. Joining of aluminum alloys has been carried out with a variety of fusion and solid state welding processes. Friction stir weld-

* Corresponding author.
Email address: tehyo_m@hotmail.com

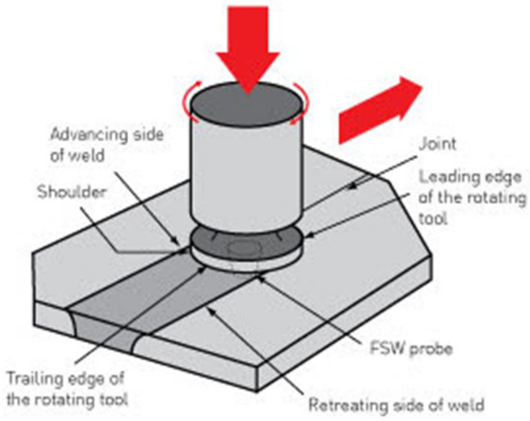

Figure 1. Schematic drawing of friction stir welding (FSW) (Liu *et al.*, 1997).

ing (FSW) was a process invented by Wayne Thomas at the Welding Institute (TWI) and the patent application was first filed in the United Kingdom in December 1991 (Thomas *et al.*, 1991). FSW as a solid-state joining technology process is one of the environmental friendly processes using frictional heat generated by rotation and traversing of the tool with a profiled pin along the butt weld joint. Figure 1 illustrates the schematic drawing of the FSW process. When frictional heat is generated materials get softened locally and plastic deformations of the work pieces occur. Tool rotation and translation expedite material flow from the front to the back of the pin and a welded joint is produced (Liu *et al.*, 1997). This method has attracted a great amount of interests in a variety of industrial applications in aerospace, marine, automotive, construction, and many others of commercial importance (Lohwasser, 2000). FSW can produce a high-quality joint compared to other conventional welding processes, and also makes it possible to join nonmetals and metals, which have been considered as non-weldable by conventional methods (Su *et al.*, 2003). The advantages of the solid-state FSW process also encompass better mechanical properties, low residual stress and deformation, weight savings, and reduced occurrence of defects (Salem *et al.*, 2002).

FSW had been carried out between conventional cast A356 and 6061-T6 aluminum alloys (Lee *et al.*, 2003). They have observed that the weld zone microstructures are dominated by the retreating side substrate. The hardness distribution was governed by precipitation of the second phase, distribution of Si particles and dislocation density. Maximum bond strength of the transition joint was close to A356 Al alloy.

Observations of FSW of dissimilar metals, namely 6061 aluminum to copper have illustrated complex flow phenomena as a consequence of differential etching of the intercalated phases producing high contrast and even high resolution flow patterns characteristic of complex (intercalation) vortices, swirls, and whorls (Murr *et al.*, 1998). However, welds in this Al:Cu systems are difficult to achieve and there is usually a large void tunnel near the weld base. There have been numerous and revealing microstructural observations in the dissimilar Al:Cu system, but systematic studies for more efficient welds should be made in other dissimilar aluminum alloy systems where differential etching can produce sufficiently high contrast to allow for flow visualization.

In this work, dissimilar joints between the recently invented SSM356-T6 aluminum alloy, which is produced by a gas induced semi-solid (GISS) process (Wannasin *et al.*, 2006) and conventional AA6061-T651 were studied. SSM356-T6 aluminum alloy was deployed to replace the use of conventional cast A356 in this study to eliminate and/or lessen the drawback properties associated with it. Welding parameters, particularly the tool rotation speeds and the welding speed, and joint properties were the main characteristics in this investigation.

2. Experimental

2.1 Materials

The base materials used for FSW in the present study were 4 mm thick plates of aluminum cast SSM356-T6 and wrought aluminum alloy AA6061-T651. Both materials are extruded medium to high strength Al-Mg-Si alloys that contain manganese to increase ductility and toughness. The T6 condition is obtained through artificial aging at a temperature of approximately 165°C. Their chemical compositions and mechanical properties are listed in Table 1. The microstructures of the base materials are shown in Figure 2. SSM

Table 1. Chemical compositions (weight%) and mechanical properties of the base materials (Bal=Balance).

Materials	Si	Fe	Cu	Mn	Mg	Zn	Ti	Cr	Ni	Al
SSM356-T6	7.74	0.57	0.05	0.06	0.32	0.01	0.05	0.02	0.01	Bal.
AA6061-T651	0.60	0.70	0.28	0.15	1.00	0.25	0.15	0.20	-	Bal.

Properties	Ultimate tensile strength (MPa)	Yield strength (MPa)	Elongation (%)
SSM356-T6	268	184	10.6
AA6061-T651	290	240	10.2

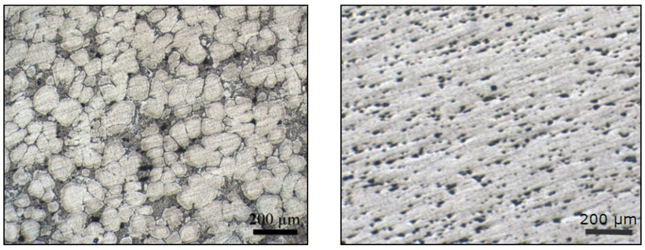

Figure 2. Microstructures of the base materials: (left) SSM356, (right) AA6061-T651.

356 exhibited a typical globular grain structure while AA 6061-T651 revealed an equiaxed structure with many etch-pits, which may be sites of second precipitate particles. The plates were cut and machined into rectangular welding specimens of 100 mm × 50 mm cross-section. A schematic diagram of FSW with sampling location is shown in Figure 3. SSM356-T6 was fixed at the advancing side and AA6061-T651 was laid on the retreating side. Both, SSM356-T6 and AA6061-T651, were rigidly clamped in order to minimize vibration and/or displacement during processing.

2.2 Welding tool size and welding parameters

A non-consumable tool made of JIS-SKH 57 tool steel was used to fabricate the joints. The cylindrical pin used as the welding tool is shown in Figure 4. The tool has a shoulder diameter, pin diameter and pin length of 20 mm, 5 mm, and 3.6 mm, respectively. The stationary welding tool rotates in clockwise direction, while the specimens, tightly clamped in position to the backing plate on the CNC machine table, traveled forward. General tool setting is when the tool pin tilts at a degree to the vertical while the machine bed is horizontal. In the CNC welding machine, however, the vertical tool pin cannot be tilted and hence an adaptation was designed and attached to the horizontal machine bed to create the required tilt angle. In this study, tool parameters were fixed at 4.4 kN of downward tool plunge force and 3° tool tilt angle. The direction of welding was normal to the rolling direction. Single pass welding procedure was adopted to fabricate the joints. Welding parameters investigated were tool rotation speed and welding speed. The values of these parameters are listed in Table 2. Three joints at two different tool rotation speed levels and six welding speeds made up a total of 36 joints (3×2×6) fabricated in this investigation.

2.3 Macro and micrographic

For the analysis of microstructural changes due to the FSW process, the joints were cross-sectioned perpendicularly to the welding direction and etched with Keller's reagent. Microstructures were acquired at different zones: transition between welded and base material, welded material, and base material. Following FSW, sections were cut from the weld zone to expose the flow pattern geometries. These sections were polished and etched using Keller's reagent. The SSM356-T6 aluminum alloy was usually most responsive to this etch and the etching difference between the SSM356-T6 aluminum alloy and AA6061-T651 aluminum alloy components could be adjusted by slight variations in composition, exposure or etching time, and temperature to produce high contrast images. Significant variations in the Keller's reagent component concentration could shift the etching preference to the AA6061-T651 aluminum alloy as well. In this way the flow patterns could be visualized by metallographic contrast under light microscopy.

2.4 Hardness and tensile strength

The Vickers hardness across the weld nugget (WN), thermo-mechanically affected zone (TMAZ) and the base

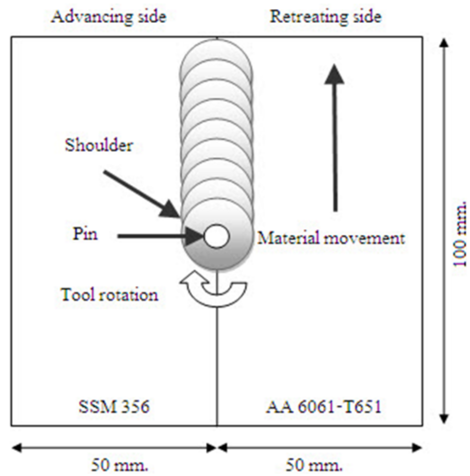

Figure 3. Schematic diagram illustrating the FSW processing. The retreating side is anti-parallel in relation to the tool rotation direction and the plate travel direction.

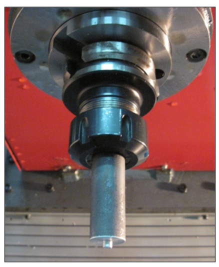

Figure 4. Illustration of the tool used in the present study.

Table 2. Welding parameters and variables.

Welding parameters	
Tool rotation speed, rpm	Welding speed, mm/min
1,750, 2,000	20, 50, 80, 120, 160, 200

materials was measured on a cross-section perpendicular to the welding direction using Vicker's microhardness tester HWDM-3 Type A at a load of 100 gf on the diamond indenter for 10 s. The hardness profiles (Figure 5) were obtained at the middle portions of the cross-section and into the base materials of the sample and were reported. The sub-size tensile test specimens with gage length 25 mm, width 6 mm, total length 100 mm and fillet radius of 6 mm were machined (Figure 6) and tested according to American Society for Testing and Materials (ASTM E8M) standard on an initial strain rate of 1.67×10^{-2} mm/s at room temperature. The tensile properties of the joint were evaluated using three tensile specimens in each condition prepared from the same joint. All specimens were mechanically polished before tests in order to eliminate the effect of possible surface irregularities.

3. Results and discussion

3.1 Macro and micrographic

Figure 7 shows a macrographic overview of the cross-section of the dissimilar friction stir welded joints of SSM 356-T6 and AA6061-T651, at the optimal condition for this experiment (tool rotation speed 2,000 rpm and welding speed 80 mm/min). Since these two aluminum alloys have different etching responses, material flows from the two sides were clearly visible in the weld nugget, which appeared to be composed of different regions of both the alloys which were severely plastically deformed. It can be seen that both materials are sufficiently stirred in the weld zone, where AA6061-T651 on the RS moves to the AS near the upper surface, while SSM356-T6 on the AS moves to the RS near the lower surface. The stir zone reveals a mixture of fine recrystallized grains of SSM356-T6 and AA6061-T651 and a double basin-shaped appearance with a zigzagged boundary between the two alloys. Combined influence of temperature and plastic deformation induced by the stirring action causes the recrystallized structure. In all FSW references on aluminum alloys, the initial elongated grains of the base materials are converted to a new equiaxed fine grain structure. This experiment confirms that behavior. The grain structure within the nugget is fine and equiaxed and the grain size is significantly smaller than that in the base materials due to the higher temperature and extensive plastic deformation by the stirring action of the tool pin. During FSW, the tool acts as a stirrer extruding the material along the welding direction. The varying rate of the dynamic recovery or recrystallization is strongly dependent on the temperature and the strain rate reached during deformation.

The welding process created a zone affected by the heat generated during the welding. The grain structure within the thermo-mechanically affected zone (TMAZ) is evident from optical microscopy observations. The structure is elongated and exhibits considerable distortions due to the mechanical action from the welding tool. Microstructural details of the dissimilar joint are presented in Figure 8. In Figure 8(a) the interface between the friction stir processes (FSP) is relatively sharp on the AS. In Figure 8(b) the boundary line between SSM356-T6 (top) and AA6061-T651 (bottom) is distinctly visible, indicating that FSW is a solid state process. In Figure 8(c) striations formed due to the tool rotation can be seen. In Figure 8(d) different zones in the mixture of the two alloys at the tool's pin edge are clearly visible.

Figure 5. Profile of the microhardness test locations.

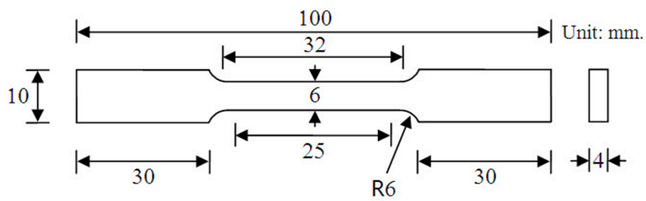

Figure 6. Dimensions of the tensile specimen according to ASTM E8M.

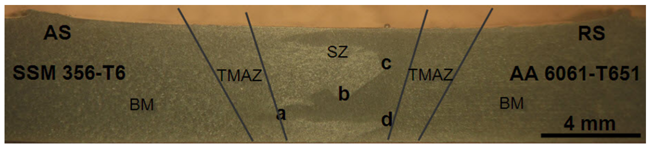

Figure 7. Macrographic of FSW of the dissimilar joint.

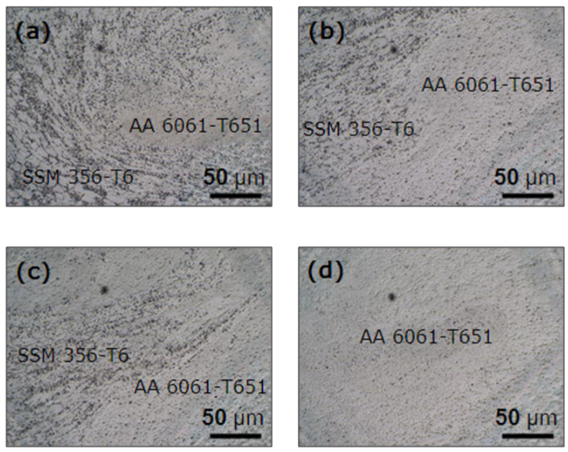

Figure 8. Micrographics of FSW of the dissimilar joint. (a), (b), (c) and (d) show schematic sequence. In (a) the interface between the friction stir processes (FSP) is relatively sharp on the AS. (b) The boundary line between SSM 356-T6 (top) and AA6061-T651 (bottom) is distinctly visible, indicating that FSW is a solid state process. (c) Striations formed due to the tool rotation can be seen and (d) different zones in the mixture of the two alloys at the tool's pin edge are clearly visible.

From the observation of FS welded, FSW was an applicable welding method and a very wide range of the welding conditions could be selected to join these dissimilar formed aluminum alloys. There is a relation between the size of the weld nugget zone and the welding speed. The movement of the tool causes an initial deformation zone to form. The area of the weld nugget zone size slightly decreased as the welding speed increased because a lower welding speed resulted in a larger welding time and consequently the weld nugget zone received more plastic deformation. The heating rate in this zone and its influence on microstructural developed is governed by (i) thermal properties of the aluminum alloy chosen and (ii) welding speed and tool rotation speed of the tool.

3.2 Hardness

Microhardness distribution data on the transverse cross-section of joints welded at all welding conditions are summarized in Figure 9. Softening is noted throughout the weld zone in the SSM356-T6 and AA6061-T651 and its average value increased with welding speed. The softening of hardness can probably be attributed mainly to the coarsening and dissolution of strengthening precipitates induced by the thermal cycle of the FSW (Muhamad *et al*., 2011). Higher hardness was observed in the WN center more than in the TMAZ. However, hardness in the SZ and TMAZ regions were slightly lower in comparison to that of the base materials. The final leg of the W-shaped profile was visualized as the microhardness values increased with increasing distance from the weld center line until base material microhardness values were reached. Away from the weld nugget, hardness levels increase up to the levels of the base materials.

3.3 Tensile strength of joints

Tensile properties and fracture locations of joints welded at different welding conditions are summarized in

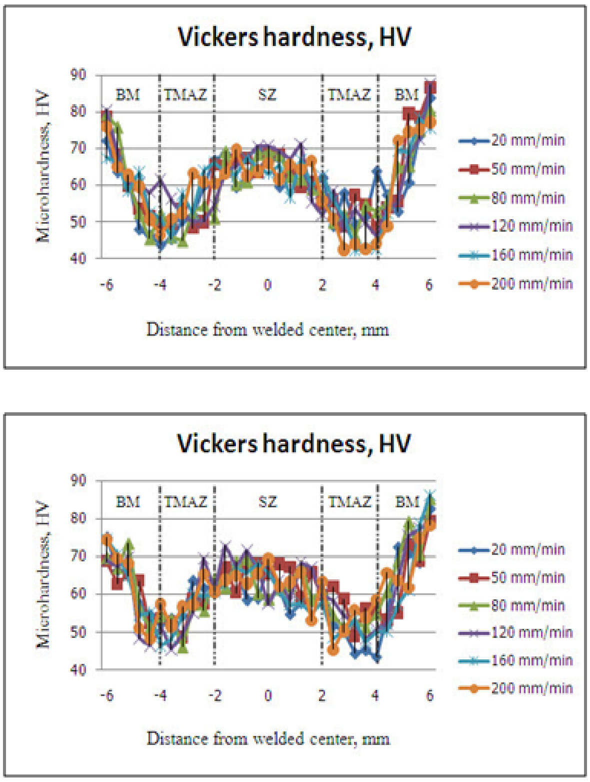

Figure 9. Microhardness profiles across the weld region at tool rotation speed 1,750 rpm (left), and 2,000 rpm (right).

Table 3. Mechanical properties and fracture locations of the welded joints in transverse direction to the weld center line.

Tool rotation speed (rpm)	Welding speed (mm/min)	Tensile properties at room temperature		
		Tensile strength (MPa)	Elongation (%)	Fracture location
1,750	20	193.5	5.071	TMAZ of SSM356-T6
	50	196.3	4.952	TMAZ of SSM356-T6
	80	192.8	5.289	TMAZ of SSM356-T6
	120	189.6	3.609	TMAZ of SSM356-T6
	160	181.1	2.389	TMAZ of AA6061-T651
	200	180.7	2.007	
2,000	20	2021	4.006	SZ
	50	205.8	5.036	TMAZ of AA6061-T651
	80	206.3	5.519	TMAZ of SSM356-T6
	120	197.2	4.563	TMAZ of SSM356-T6
	160	198.7	4.748	SZ
	200	194.7	3.224	SZ

Table 3. From the investigation, the higher tool rotation speed leads to a higher tensile strength. A maximum average tensile strength value of 206.3 MPa was attained for a joint produced at the tool rotation speed of 2,000 rpm and the welding speed of 80 mm/min. Tensile properties of FSW butt joints of SSM356-T6 plate and AA6061-T651 plate depend mainly on welding defects and hardness of the joint. Fractures occurred at the TMAZ and SZ of SSM356-T6 in case of defect-free joints. However, fractures occurred in the SZ for joints consisting of defects.

Equation 1 (Kim *et al.*, 2006) outlines the relationships between heat input, pressure, tool rotation speed, welding speed, and other factors. In tool rotation speed versus tensile strength of the welded joints, at the lower tool rotation speed (1,750 rpm) frictional heat generated was less, resulting in poor plastic flow of the materials being welded and thus lower tensile strength values were observed. At higher tool rotation speed (2,000 rpm) metallurgical transformation such as solubilization, re-precipitation, coarsening and strengthening precipitated in the weld zone, lowering the dislocation density (Threadgill, 1997; Benavides *et al.*, 1999; Lomolino *et al.*, 2005) and increased the tensile strength of the welded joints. Variation in tensile strengths at different tool rotation speed was due to different material flow behavior and frictional heat generated. The maximum tensile strength of the dissimilar FS welded joint was obtained under a welding speed of 50 mm/min for the tool rotation speed of 1,750 rpm, and a welding speed of 80 mm/min for the tool rotation speed of 2,000 rpm.

$$Q = \frac{4\pi^2 \alpha\mu PNR^3}{3V} \tag{1}$$

where Q is the heat input per unit length (J/mm), α is the heat input efficiency, μ is the friction coefficient, P is the pressure (N), N is the tool rotation speed (rpm), R is the radius of the shoulder (mm), and V is the welding speed (mm/min).

An increase in the welding speed resulted in an increase in the tensile strength of the weld. The tensile strength reaches a maximum value, but a further increase in the welding speed beyond that resulted in a decrease of the tensile strength of the weld. At the lowest welding speed (20 mm/min), as well as the highest welding speed (200 mm/min), lower tensile strengths were observed. The lowest welding speed generated high heat input and encouraged metallurgical transformations of the weld zone leading to a lower tensile strength. The highest welding speed discouraged clustering effect of strengthening precipitates, plastic flow of materials (Flores *et al.*, 1998, Murr *et al.*, 1998, Sato, 2003, Su *et al.*, 2003, Srivatsan *et al.*, 2007), and localization of strain (Srivatsan *et al.*, 2007) due to insufficient frictional heat generated (Colligan *et al.*, 2003; Shanmuga *et al.*, 2010).

The relationship between macrostructures and tensile strength of FS welded is as following. From Figure 7 it can be seen that the macrostructures at following conditions, 2,000 rpm, 80 mm/min, show maximum tensile strength found that macrostructure structure of weld metal had the most completely altogether at the area as dept of tool pin could be seen clearly from weld range. So that showed FSW on condition weld range with had maximum tensile was well completely seepage altogether, had enough melting in dept of tool pin.

And macrostructure structure of condition on minimum tensile strength found that macrostructure of weld metal had the most completely altogether at the phase as dept of tool pin could be seen clearly from weld range. So that showed Friction Stir Welding on sample weld range with had minimum tensile strength was well completely seepage altogether, had enough melting in dept of tool pin phase but hole which was result from melting welding of two materials that had not enough flowed melting and also had the heat reacted with weld range while welding. That made weld range was not completely and occurred hole, because the samples which used in welding experimental were two materials that be different grade and chemical property made altogether welding. A hole which occurred was hole from FSW of sample on AA6061-T651 side, which occurred lower melting than SSM356-T6.

Conclusion

In the present study, SSM356-T6 and AA6061-T651 aluminum alloys joined by FSW under two different tool rotation speeds and six welding speeds were investigated. Summarizing the main features of the results, following conclusions can be drawn:

1. The microstructures of dissimilar-formed SSM 356-T6 and AA6061-T651 joints revealed that recrystallized mixed structures of two materials can be easily identified by etching responses of both materials in the stir zone. The relation between the size of the weld nugget zone and welding speed. The area of the weld nugget zone size slightly decreased as the welding speed increased.

2. Hardness observed in the weld center was higher than that in the TMAZ. However, hardness in all regions was less comparing with the base materials. The final leg of the W-shaped Vickers hardness profile on the cross section increased with increasing distance from the weld center line to the value of the base materials.

3. An increase in the welding speed apparently lead to an increase in the tensile strength of the specimen. In fact, the tensile strength approached a maximum value close to the lesser of the parent base materials then decreased with increasing welding speed on the dissimilar FS welded specimens. Thus, neither a too low welding speed (below 80 mm/min) nor a too high welding speed (beyond 80 mm/min) is desirable.

4. In this study, a higher tool rotation speed of 2,000 rpm resulted in a higher tensile strength of the FS welded specimen. A maximum average tensile strength value of 206.3 MPa was recorded for a joint fabricated at the tool rotation speed of 2,000 rpm and at a welding speed of 80 mm/min.

Acknowledgments

This research was supported by research funds from the Faculty of Engineering, Princess of Naradhiwas University, and from the Graduate School, Prince of Songkla University.

References

Benavides, S., Li, Y., Murr, L.E., Brown, D. and McClure, J.C. 1999. Low temperature Friction Stir welding of 2024 aluminum. Scripta Materialia. 41(8), 809-815.

Colligan, J., Paul, J., Konkol, James, J., Fisher and Pickens Joseph, R. 2003. Friction stir welding demonstrated for combat vehicle construction. Welding Journal. 1-6.

Flores, O.V., Kennedy, C., Murr, L.E., Brown, D., Pappu, S. and Nowak, B.M. 1998. Microstructural issues in a friction-stir-welded aluminum alloy. Scripta Materialia. 38(5), 703-708.

Kim, Y.G., Fujii, H., Tsumura, T., Komazaki, T. and Nahata, K. 2006. Three defect types in friction stir welding of aluminum die casting alloy. Materials Science and Engineering A. 415, 250-254.

Lee, W.B., Yeon, Y.M. and Jung, S.B. 2003. The joint properties of dissimilar formed Al alloys by friction stir welding according to the fixed location of materials. Scripta Metallurgica. 49, 423-428.

Liu, G., Murr, L.E., Niou, C., McClure, J.C. and Vega, F.R. 1997. Microstructural Aspects of the Friction Stir Welding of 6061-T6 Aluminum. Scripta Metallurgica. 37, 355-361.

Lohwasser, D. 2000. Proceedings of the 2nd International Symposium on Friction Stir Welding, Gothenburg, Sweden.

Lomolino, S., Tovo, R. and dos Santos, J. 2005. On the fatigue behavior and design curves of friction stir butt welded Al alloys. International Journal of Fatigue. 27, 305-316.

Muhamad, T., Prapas, M. and Somchai, C. 2011. Friction stir welding of dissimilar joint between semi-solid metal 356 and AA6061-T651 by computerized numerical control machine. Songklanakarin Journal of Science and Technology. 33(4), 441-448.

Murr, L.E., Ying Li., Flores, R.D., Elizabeth, A., Trillo and McClure, J.C. 1998. Intercalation vortices and related microstructural features in the friction stir welding of dissimilar metals. Materials Research Innovations Journal. 2, 150-163.

Murr, L.E., Liu, G. and Mc Clure, J.C. 1998. A TEM study of precipitation and related microstructures in friction-stir-welded 6061 aluminum. Journal of Materials Science and Engineering. 33(5), 1243-1251.

Salem, H.G., Reynolds, A.P. and Lyons, J.S. 2002. Microstructure and retention of superplasticity of friction stir welded superplastic 2095 sheet. Scripta Materialia. 46, 337-342.

Sato, Y.S., Urata, M., Kokawa, H. and Ikeda, K. 2003. Hall-petch relationship in friction stir welds of equal channel angular-pressed aluminum alloys. Materials Science and Engineering A. 354, 298-305.

Shanmuga Sundaram, N. and Murugan, N. 2010. Tensile behavior of dissimilar friction stir welded joints of aluminum alloys. Materials and Design. 31, 4184-4193.

Srivatsan, T.S., Satish, V. and Lisa P. 2007. The tensile deformation and fracture behavior of friction stir welded aluminum alloy 2024. Materials Science and Engineering A. 466, 235-245.

Su, J.Q., Nelson, T.W., Mishra, R. and Mahoney, M. 2003. Microstructural investigation friction stir welded 7050-T651 aluminum. Acta Materialia. 51, 713-729.

Threadgill, P. 1997. Friction stir welds in aluminum alloys preliminary microstructural assessment, TWI Bulletin - The Welding Institute, Abington, U.K., Industrial Report No: 513/2/97.

Thomas, W.M., Nicholas, E.D., Needham, J.C., Murch, M.G., Templesmith, P. and Dawes, C.J. 1991. Friction Stir Welding, International Patent Application No. PCT/GB 92102203 and Great Britain Patent Application No. 9125978.8.

Wannasin, J., Martinez, R.A. and Flemings, M.C. 2006. A Novel Technique to Produce Metal Slurries for Semi-Solid Metal Processing. Solid State Phenomena. 116-117, 366-369.